Proceedings in MANUFACTURING SYSTEMS

Proceedings in Manufacturing Systems, Volume 7, Issue 3, 2012 ISSN 2067-9238

MODELING AND PERFORMANCE ANALYSIS OF A SPINDLE ELECTRIC DRIVE WITH ADAPTIVE SPEED CONTROL

Mikho MIKHOV[1,*], Marin ZHILEVSKI[2], Alexander SPIRIDONOV[3]

[1)] Assoc. Prof., Eng, PhD, Faculty of Automatics, Technical University of Sofia, Bulgaria
[2)] MSc, Eng, Faculty of Automatics, Technical University of Sofia, Bulgaria
[3)] Eng, Faculty of Automatics, Technical University of Sofia, Bulgaria

Abstract: *The performance of a DC electric drive system with dual-zone speed regulation is discussed in this paper. The controlled object consists of a four-quadrant power converter for armature voltage, a nonreversible power converter for field voltage and a separately excited DC motor. The motor speed is regulated at constant magnetic flux in the first zone, while in the second zone the flux is reduced at constant armature voltage. The speed zone switching is a function of armature voltage of the motor. Controllers have been synthesized for the regulated variables of motor speed, armature current and field current. To improve the electric drive performance an adaptive speed controller with switchable structure is offered. In the second zone the controller parameters adapt to the decreasing magnetic flux. To verify the offered control algorithm functionality appropriate computer simulation models have been developed, using the MATLAB/SIMULINK software package. Detailed study and analysis by means of modelling and computer simulation have been carried out for different loads at the respective transient and steady state regimes. The analysis shows that such a driving system can ensure good performance. The developed models and the results obtained could be used in optimization and final set up of such types of speed control driving systems.*

Key words: *speed control, dual-zone regulation, modelling, computer simulation, performance analysis.*

1. INTRODUCTION

The machines under consideration relate to a class of milling machines with multi-coordinate electric drive systems. Spindle is the fourth coordinate axis which puts the following requirements:

- dual-zone speed regulation;
- oriented suspension with high accuracy;
- reversing of speed and motor torque.

Dual-zone speed control is often required in industrial automation. Regulation is carried out at constant motor torque until a basic speed level is reached. After that, it is carried out at constant power. The rated speed is most often regarded as basic speed value.

With DC electric drives the speed is regulated at constant magnetic flux in the first zone, while in the second zone the flux is reduced at constant back electromotive force (EMF) voltage or armature voltage. Automatic switching of the two speed areas is realized as a function of one of these variables.

A feature of the dual-zone speed control is that the drive system structure changes along the process of regulation and the optimal coordination of zones creates the main control problem.

In [1] a DC electric drive system with dual-zone speed regulation is presented, where control shift is a function of the motor back EMF voltage. Using an appropriate vector-matrix description of the controlled object, in [2] an optimal modal speed controller for the first zone is synthesized, as well as an adaptive optimal modal controller of the back EMF voltage for the second zone. Adaptive speed control of DC electric drives with thyristor converters is described in [3].

Mathematical modelling and computer simulation offer effective ways to study the electric drive systems in details, in various dynamic and static working regimes, especially when it is not possible or it is inconvenient to carry out such tests in laboratory or industrial environments [4].

This paper discusses DC electric drive systems with dual-zone speed regulation, where control shift is a function of the armature voltage. The controlled object under consideration includes a thyristor four-quadrant power converter for armature voltage, a thyristor nonreversible power converter for field voltage and a separately excited DC motor.

To improve the electric drive performance an adaptive speed controller with switchable structure is developed. In the second zone the controller parameters adapt to the decreasing magnetic flux. Such an approach provides for better static and dynamic characteristics of the driving system.

Through modelling and computer simulation, operation in the transient and steady state regimes has

[*] Corresponding author: Technical University of Sofia, 8 Kliment Ohridski Blvd., 1000 Sofia, Bulgaria;
Tel.: +359 2 965 29 46;
E-mail addresses: *mikhov@tu-sofia.bg* (M. Mikhov), *electric_zhilevski@abv.bg* (M. Zhilevski), *aspiridonov@abv.bg* (A. Spiridonov)

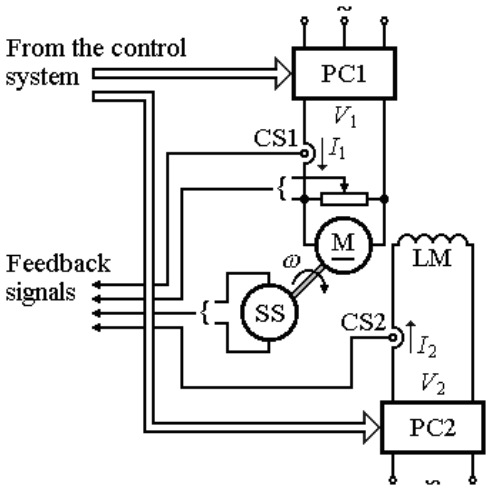

Fig. 1. The controlled object under consideration.

been analyzed, at various loads and disturbances applied to the motor shaft.

Some results from this research in respective motor speed areas are presented.

2. FEATURES OF THE DRIVE SYSTEM

The controlled object configuration is presented in Fig. 1, where the next notations are used: *PC*1 – armature voltage power converter; *PC*2 – field voltage power converter; *M* – *DC* motor; *LM* – field coil; *CS*1 – armature current sensor; *CS*2 – field current sensor; *SS* – speed sensor; V_1 – armature voltage; V_2 – field voltage; I_1 – armature current; I_2 – field current; ω – motor speed.

If the electric drive system should be four-quadrant with both armature current and speed reversion, the power converter for armature voltage is of reversive type, while the power converter for the field voltage is non-reversive.

The drive system block diagram is shown in Fig. 2, where the following notations are used: V_{sr} – speed reference signal; V_{sf} – speed feedback signal; $G_{sc}(s)$ – transfer functions of the speed controller; K_{sf} and τ_{sf} – gain and time-constant of the speed feedback; CLB – current limitation block; V_{c_1r} – armature current reference signal; V_{c_1f} – armature current feedback signal; $G_{c_1c}(s)$ – transfer function of the armature current controller; K_{p_1} and τ_{p_1} – gain and time-constant of the armature voltage power converter; K_{c_1f} and τ_{c_1f} – gain and time-constant of the armature current feedback; R_{1_Σ} – armature circuit resistance; τ_{1_Σ} – armature circuit time-constant; c – motor coefficient; E - back EMF voltage; $V_{\varphi r}$ – magnetic flux reference signal; $G_{c_2c}(s)$ – transfer function of the field current controller; SB – switching block; $|V_{v_1f}|$ – armature voltage feedback signal; V_{c_2f} – field current feedback signal; K_{p_2} and τ_{p_2} – gain and time-constant of the field voltage power converter; AVB – absolute value block; K_{v_1f} – gain of the armature voltage feedback; R_{2_Σ} – field circuit resistance; τ_{2_Σ} – field circuit time-constant; K_{c_2f} and τ_{c_2f} – gain and time-constant of the field current feedback; K_Φ – coefficient of the magnetic flux curve gradient; Φ – magnetic flux; T – motor torque; T_l – load torque applied to the motor shaft; J_Σ – total inertia referred to the motor shaft.

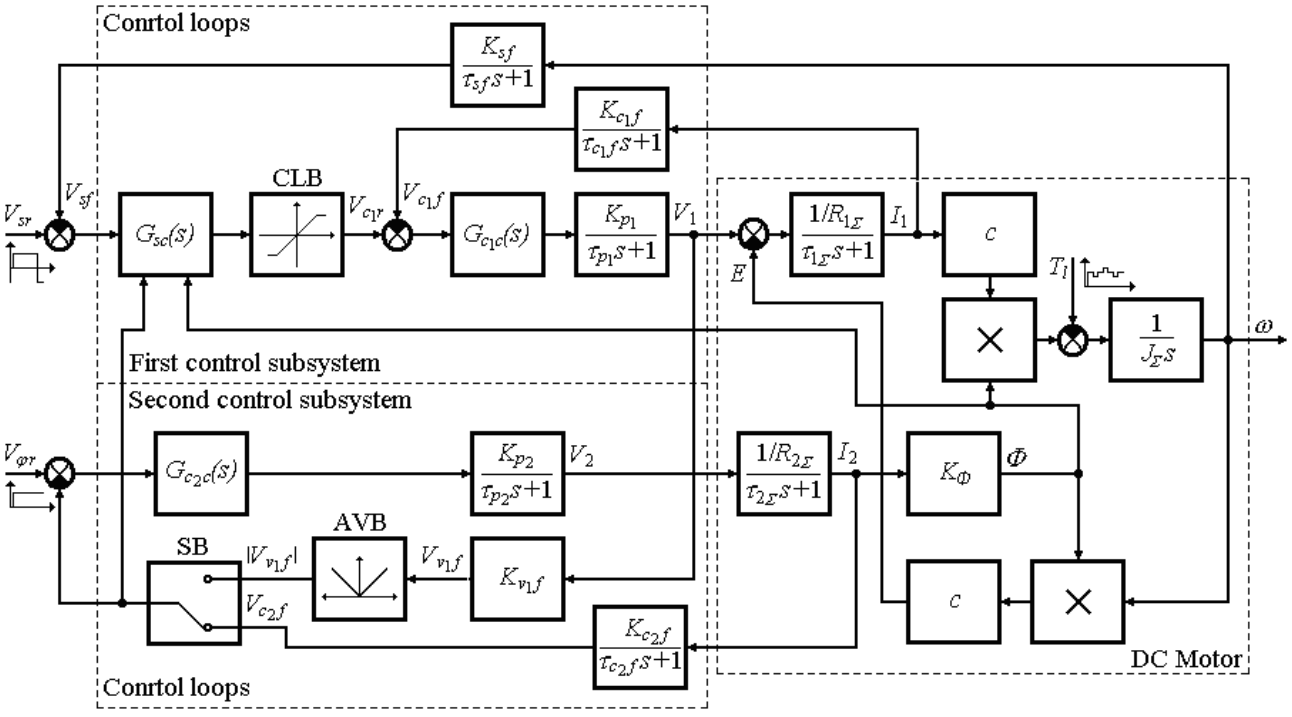

Fig. 2. Block diagram of the electric drive system.

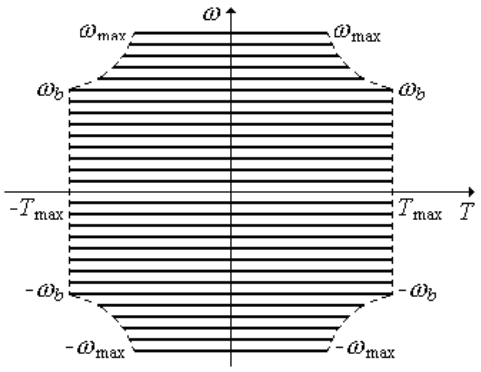

Fig. 3. Speed/torque curves of the four-quadrant drive system.

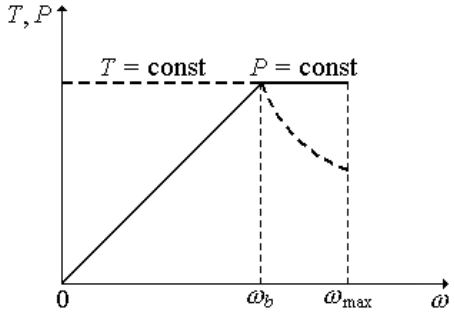

Fig. 4. Torque/speed and power/speed diagrams.

Motor speed regulation until the voltage value of $V_1 \le V_b$ is carried out at rated magnetic flux $(\Phi = \Phi_{rat})$, at the expense of the armature voltage change. At $V_1 > V_b$ the regulation is done through the flux reduction $(\Phi < \Phi_{rat})$. Within the entire range, speed is set up by the control signal V_{sr}.

Figure 3 shows speed/torque characteristics of the four-quadrant electric drive system, where ω_{max} is the upper bound of the speed regulation range and T_{max} is the maximum motor torque. At $\omega_r > \omega_b$ field cuttent in steady state regime is $I_2 < I_{2rat}$, while the admissible armature current is limited below the I_{1max} value.

Speed control is realized at constant motor torque until the basic speed level ω_b is reached. After that, it is carried out at constant power. The torque/speed and power/speed diagrams are presented in Fig. 4.

3. MODELING OF THE DRIVE SYSTEM

Using the MATLAB/SIMULINK software package some computer simulation models have been developed for systems with dual-zone speed regulation to verify the respective control algorithms.

The main parameters of the controlled object are presented in Table 1. Some of them are specified experimentally.

A simplified model of the dual-zone drive system under consideration is illustrated in Fig. 5, where the next notations are used: *SC* and *CL* – speed controller and armature current limiter; *CC*1 – armature current controller; *PC*1 – armature power converter; *CC*2 – field current controller; *PC*2 – field power converter; *SB* – switching block; *AVB* – absolute value block.

The control system includes two subsystems, the input signals of which are for setting of speed and magnetic flux respectively.

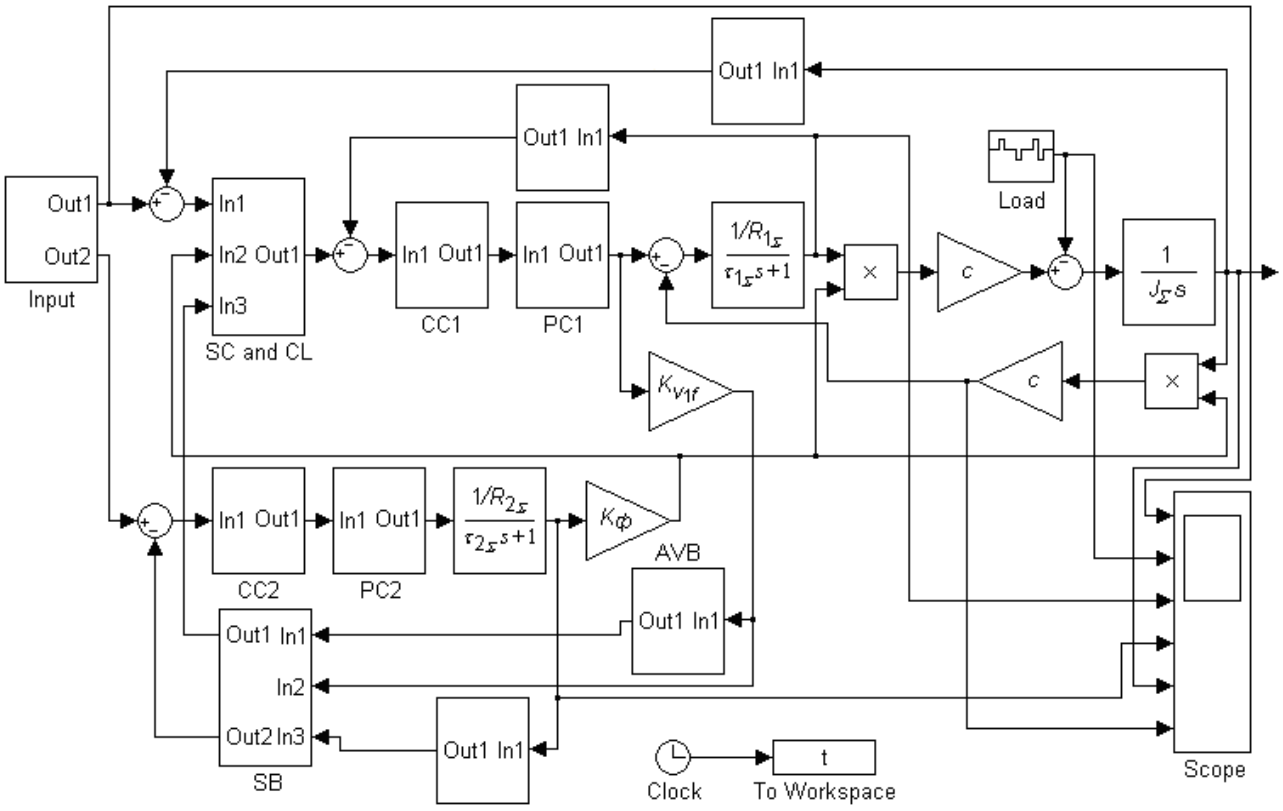

Fig. 5. Model of the dual-zone electric drive system.

Table 1

Main parameters of the controlled object

Parameter	Value
Rated power	3.4 kW
Rated armature voltage	220 V
Rated armature current	17.6 A
Rated speed	314 rad/s
Back EMF voltage coefficient	0.6737 Vs/rad
Torque coefficient	0.6737 Nm/A
Armature circuit resistance	1.64 Ω
Armature inductance	0.027 H
Total inertia referred to the motor shaft	0.074 kg.m^2
Time-constant of the armature converter	0.004 s
Gain of the armature power converter	24.04
Armature circuit time-constant	0.0165 s
Time-constant of the field converter	0.005 s
Gain of the field power converter	22.1
Field circuit time-constant	0.11 s

The first subsistem is of dual-loop type, with subordinated regulation. Control loops opitimization is carried out following the resepctive critera, providing for the necessary performnce [5, 6]. Tuning of controllers is done sequentially, starting from the inner loop.

The transfer function of the armature current controller is expressed as follows:

$$G_{c_1c}(s)=\frac{R_{1_\Sigma}\left(\tau_{1_\Sigma}s+1\right)}{a_{c_1}K_{p_1}K_{c_1f}\tau_{\mu c_1}s}, \qquad (1)$$

where a_{c_1} is a coefficient influencing the armature current loop dynamic characteristics; $\tau_{\mu c_1}=\tau_{p_1}+\tau_{c_1f}$ – summary small time-constant of this loop, not subject to compensation; $\tau_{1\Sigma}=L_{1_\Sigma}/R_{1_\Sigma}$ – armature circuit time-constant; L_{1_Σ} – armature inductance.

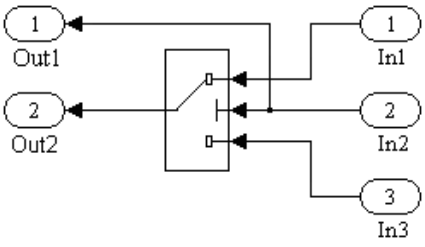

Fig. 6. Model of the switching block.

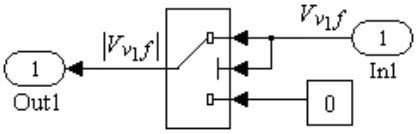

Fig. 8. Model of the absolute value block.

One of the used versions for the first subsystem external loop optimization leads to the following transfer function of the speed controller:

$$G_{sc}(s)=\frac{J_\Sigma K_{c_1f}}{a_sK_{sf}\tau_{\mu s}K_e}\left(1+\frac{1}{a_s^2\tau_{\mu s}s}\right)= \\ =K_{sc}\left(1+\frac{1}{\tau_{sc}s}\right)=f(\Phi), \qquad (2)$$

where: a_S is a coefficient influencing the speed loop dynamic characteristics; $\tau_{\mu s}=a_{c_1}\tau_{\mu c_1}+\tau_{sf}$ – summary small time-constant of this loop, not subject to compensation; $K_e=c\Phi$ – back EMF voltage coefficient; K_{sc} and τ_{sc} – gain and time-constant of the speed controller.

In the second zone the magnetic flux changes and to improve the electric drive performance an adaptive speed controller with switchable structure has been synthesized. In this zone the controller parameters adapt to the decreasing magnetic flux. Adaptation to flux change starts after the zone switching, which takes place at the specified base value of the armature voltage $V_1=V_{1b}$.

The respective switching block model is presented in Fig. 6.

A block diagram of the adaptive speed controller is shown in Fig. 7. The structure shift is realized though a signal from the switching block of SB.

The transfer function of the field current controller is described by this equation:

$$G_{c_2c}(s)=\frac{R_{2_\Sigma}\left(\tau_{2_\Sigma}s+1\right)}{a_{c_2}K_{p_2}K_{c_2f}\tau_{\mu c_2}s}, \qquad (3)$$

where a_{c_2} is a coefficient influencing the field current loop dynamic characteristics; $\tau_{\mu c_2}=\tau_{p_2}+\tau_{c_2f}$ – summary small time-constant of this loop, not subject to compen-

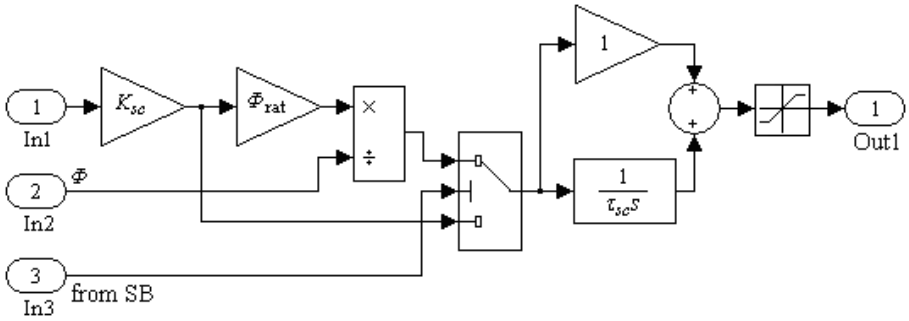

Fig. 7. Model of the adaptive speed controller and current limiter.

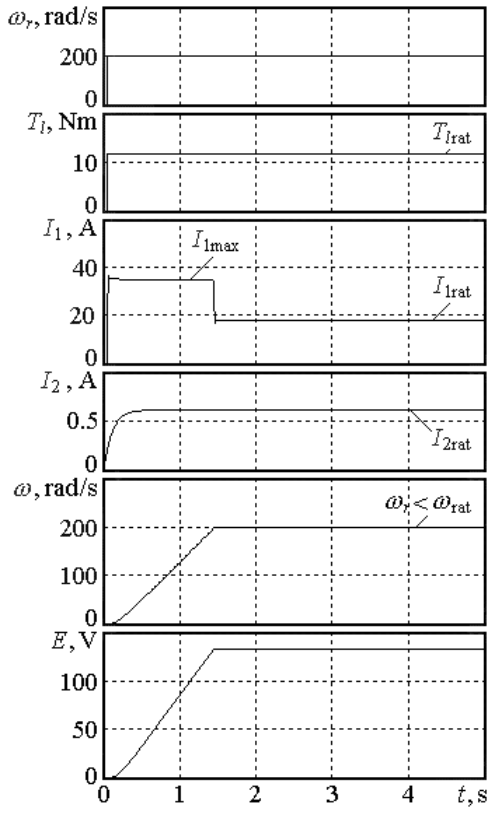

Fig. 9. Time-diagrams for the first zone of speed regulation.

sation; $\tau_{2\Sigma} = L_{2\Sigma}/R_{2\Sigma}$ – field circuit time-constant; $L_{2\Sigma}$ – field inductance.

If motor speed direction changes, the feedback signal sign $V_{v_1 f}$ changes, but the $|V_{v_1 f}|$ signal remains with the same sign (positive). For that reason, to avoid the $V_{v_1 f}$ sign influence, in four-quadrant drive systems an absolute value block AVB is included. The model of this block is presented in Fig. 8.

The models developed allow detailed studies of the dual-zone drive system by means of computer simulation in the respective dynamic and static regimes at diverse loading, disturbances and work conditions.

4. SIMULATION RESULTS AND ANALYSIS

Figure 9 shows some time-diagrams, obtained for the first zone of speed regulation. The transient start process is shown, as well as operaton at steady state regime with rated load torque applied to the motor shaft. The presented characteristics are as follows: speed reference $\omega_r(t)$; load torque $T_l(t)$, armature current $I_1(t)$, field current $I_2(t)$, motor speed $\omega(t)$ and back EMF voltage $E(t)$.

For normal operation of the electric drive system the field power converter is switched before the armature power converter. The set motor speed is $\omega_r < \omega_{rat}$ and the starting armature current is limited to the maximum admissible value of $I_{1\max}$, which provides a maximum starting motor torque. The field current is of a consntant value of $I_2 = I_{2\text{rat}}$.

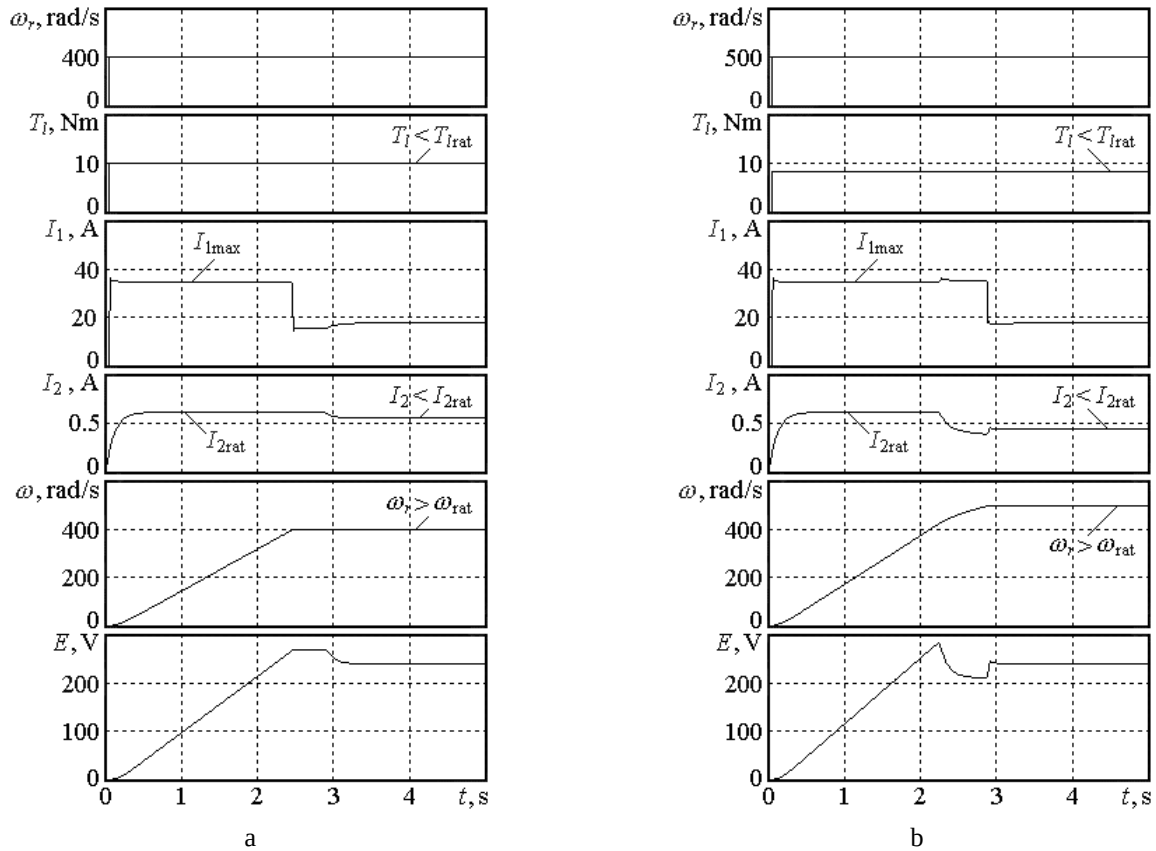

Fig. 10. Time-diagrams for the second zone of speed regulation.

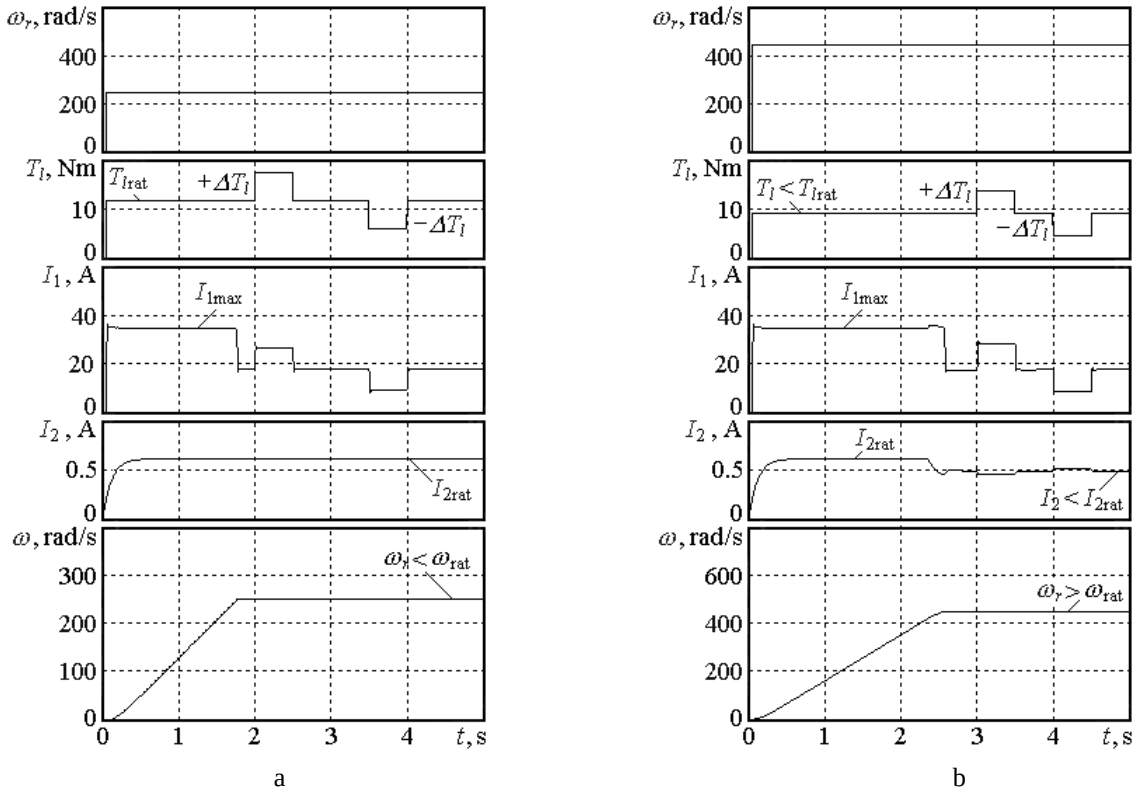

Fig. 11. Stabilization of the motor speed in presence of disturbances.

Figure 10 illustrates the drive performance in the zone with flux weakening. The same variables as those in Fig. 9 are shown. These time-diagrams are obtained for two reference motor speeds respectively: 400 rad/s (Fig. 10a) and 500 rad/s (Fig. 10b).

Figure 11 presents speed stabilization in the presence of disturbances. The system reaction is shown with respect to armature current I_1, field current I_2 and motor speed ω. The time-diagrams are obtained for two set motor speeds: 250 rad/s (Fig. 11a) and 450 rad/s (Fig. 11b). The load torque is equal to the respective value T_l, while the disturbances applied sequentially are $+\Delta T_l = 0.5T_l$ and $-\Delta T_l = -0.5T_l$ respectively. As evident, with an appropriate tuning of the speed controller, static speed error does not appear when T_l changes. At higher speeds the load torque applied is smaller due to decreasing of motor torque in the second zone.

5. CONCLUSIONS

Computer simulation models of electric drive systems with dual-zone speed regulation have been developed allowing study at various loads and disturbances applied to the motor shaft.

Appropriate controllers to regulate motor speed, armature current and field current have been synthesized. Optimization of the respective control loops by different criteria has been carried out.

To improve the electric drive characteristics an adaptive speed controller with switchable structure is offered. In the second zone the controller parameters adapt to the decreasing magnetic flux.

Analysis of the dynamic and static regimes of operation has been carried out showing that such a driving system can ensure good performance.

The simulation models and the results obtained can be used as in optimization and set up of the dual-zone drive systems discussed above, so as illustration in the process of teaching about such types of electric drives.

REFERENCES

[1] M. Mikhov, B. Balev, *Modeling and optimization of an electric drive system with dual-zone speed regulation*, International Conference on Communication and Energy Systems and Technologies, B. Milovanovic (Ed.), pp. 575–578, Nish, Serbia, June 29–July 2005, UNIGRAF, Nish.

[2] M. Mikhov, Ts. Georgiev, *An Approach to Synthesis of a Class of Electric Drives with Dual-Zone Speed control*, Advances in Electrical and Computer Engineering, Vol. 10, No. 4, 2010, pp. 87–94.

[3] U. Keuchel, V. Stephan, *Microcomputer-Based Adaptive Control Applied to Thyristor-Driven DC Motors*, Springer-Verlag, London, 1994.

[4] C. Ong, *Dynamic simulation of electric machinery*, Prentice Hall, New Jersey, 1998.

[5] M. Mohan, *Electric drives – an integrative approach*, MNPERE, Minneapolis, 2003.

[6] I. Boldea, S. A. Nasar, *Electric drives*, CRC, Boca Raton, 2006.